POUDRETTEITE: A RARE GEM SPECIES FROM THE MOGOK VALLEY

By Christopher P. Smith, George Bosshart, Stefan Graeser, Henry Hänni, Detlef Günther, Kathrin Hametner, and Edward J. Gübelin

In 2000, an unfamiliar gemstone was purchased in Mogok. It subsequently proved to be the rare borosilicate poudretteite, a mineral that previously had been identified only as tiny crystals from Mont Saint-Hilaire, Quebec, Canada. This article presents a complete gemological description of this unique gemstone and furthers the characterization of this mineral by advanced spectroscopic and chemical analytical techniques.

The Mogok Valley in the Shan State of upper Myanmar (Burma) is a region rich in history, tradition, lore, and gems. Myanmar is commonly referred to as the world's premier source of ruby, sapphire, spinel, peridot, and jadeite. In addition, the Mogok Stone Tract plays host to a wide range of other notable gem species and varieties, including amethyst, andalusite, danburite, garnet, goshenite, scapolite, topaz, tourmaline, and zircon. It has also produced a number of very rare gems, such as sinhalite, colorless chrysoberyl, taaffeite, and painite (see, e.g., Kammerling et al., 1994; Themelis, 2000).

In November 2000, an Italian dealer buying gems in Mogok was shown a 3 ct faceted gemstone (figure 1) that the local gem merchant/gemologist could not identify (F. Barlocher, pers. comm., 2000). This gemstone was subsequently submitted to the Gübelin Gem Lab for examination and identification. On the basis of the results given in this article, it proved to be the first documented gem-quality specimen of poudretteite, a mineral that has been reported previously from only one source in the province of Quebec, Canada (Grice et al., 1987), and only in small numbers and sizes (see below). These results were also given to R. Schlüssel, who subsequently included poudretteite in his book on Mogok (Schlüssel, 2002). This extremely rare sample permits the first comprehensive gemological description of this material and expansion of the body of analytical data for this mineral by a variety of techniques that had not been used previously.

BACKGROUND

The first description of the mineral poudretteite was published by Grice et al. (1987), with additional original data subsequently provided by Hawthorne and Grice (1990). Just seven crystals were discovered at Mont Saint-Hilaire, Rouville County, Quebec, Canada, during the mid-1960s. However, these specimens were not recognized and registered as a new mineral until July 1986 (J. Grice, pers. comm., 2001). The mineral was named after the Poudrette family, who owned and operated the Carrière R. Poudrette, the quarry on Mont Saint-Hilaire that produced the crystals. Until now, these were the only specimens of poudretteite known to exist.

Grice et al. (1987) reported that the poudretteite occurred in marble xenoliths within a nepheline syenite breccia, associated with pectolite, apophyllite, and minor aegirine. The crystals were found to be $KNa_2B_3Si_{12}O_{30}$ and were described as colorless to very pale pink, roughly equidimensional, deeply

See end of article for About the Authors and Acknowledgments.
Article submitted November 12, 2001.
GEMS & GEMOLOGY, Vol. 39, No. 1, pp. 24–31.

etched, barrel-shaped hexagonal prisms measuring up to 5 mm in longest dimension.

Poudretteite was referred to as a new member of the "osumilite group" by Grice et al. (1987); osumilite itself was first described in 1956. Because milarite (described in 1870) is the prototype mineral for the large structural group that includes osumilite, for historical reasons some came to prefer the term *milarite group* (e.g., Hawthorne and Grice, 1990; Hawthorne et al., 1991). Yet Clark (1993) and Mandarino (1999) continued to use the term *osumilite group*. Inasmuch as both group names are currently used in the mineralogical literature, and until there is unanimity in mineralogical terminology, we will refer to poudretteite as belonging to the osumilite/milarite group.

There are 17 minerals in the osumilite/milarite group (Mandarino, 1999). Of these, only sugilite is familiar to most gemologists (see, e.g., Shigley et al., 1987). Sogdianite, another mineral in this group, has also been encountered, though rarely, in gem quality (Bank et al., 1978; Dillmann, 1978).

Figure 1. This extremely rare 3.00 ct poudretteite was recovered recently from the Mogok Valley of upper Myanmar. Previously, only small crystals of poudretteite had been found during the 1960s in the Mont Saint-Hilaire syenite complex of Quebec. Photo by Phillip Hitz.

ANALYTICAL METHODS

We used standard gemological techniques to record the refractive indices (with a sodium vapor lamp), birefringence, optic character, pleochroism, specific gravity (by the hydrostatic method), absorption spectra (with a desk-model spectroscope), and reaction to long- and short- wave ultraviolet radiation (with a combination 365 nm and 254 nm lamp). The internal features were studied with binocular microscopes and fiber-optic and other illumination techniques. To analyze the internal growth structures, we used a horizontal microscope, a specially designed stone holder, and a mini-goniometer contained in one of the oculars of the microscope, employing the methods described by Kiefert and Schmetzer (1991) and Smith (1996).

Identification of the gemstone as poudretteite was done by X-ray diffraction analysis, performed with a Debye-Scherrer camera that was 90 mm in diameter and used FeK radiation. Film shrinkage was corrected using a quartz standard. The powder pattern was indexed applying the program by Benoit (1987), and lattice parameters were refined after Holland and Redfern (1997).

To record the UV, visible, and near-infrared absorption spectra (200–2500 nm), we used a Perkin Elmer Lambda 19 dual-beam spectrometer, equipped with beam condensers and polarizers (Polaroid HNP`B filters for the 270–820 nm range, and a calcite polarizer with a goniometer scale for the 820–2500 nm range). The region from 200 to 270 nm was recorded in unpolarized light. For the 200–820 nm range, the spectra were run at a speed of 1 nm/sec and with a spectral slit width of 0.5 nm. For the 820–2500 nm range, the scan speed was increased to 2 nm/sec with a slit width automatically adjusted to the recorded signal intensity.

We also used two other methods for infrared spectrometry. First, a minute scraping of powder from the gemstone (<0.001 ct) was admixed to >100 parts of dry KBr salt, ground together in an alumina mortar, evacuated, and pressed to form a transparent pellet 5 mm in diameter. We collected the mid-infrared spectrum of the pellet using a dispersive Perkin Elmer 883 spectrometer in the region between 4000 and 250 cm^{-1}, thus connecting the end of the near-infrared region at 2500 nm (4000 cm^{-1} is equivalent to 2500 nm). Second, we analyzed the 3 ct gemstone itself in the 7000–400 cm^{-1} region with a Pye-Unicam 9624 Fourier-transform infrared (FTIR) spectrometer and a Specac 5× beam condenser, recording 200 scans at 4 cm^{-1} resolution. In the absence of polarization accessories, mid-infrared spectra were taken in beam directions oriented nearly parallel (||) and perpendicular (^) to the optic axis of the gemstone. The two methods were used because gemstones measuring several millimeters in thickness, when recorded in the transmission mode (e.g., with a beam condenser), show total absorption

below about 2000 cm^{-1} but very strongly enhanced absorption characteristics above 2000 cm^{-1}, whereas the KBr pellet will produce spectra in the region below 2000 cm^{-1} (the fingerprinting region) but very little detail above that. The reason for this is the extreme difference in optical path length of the IR beam through the pulverized sample in a KBr pellet (on the order of 1 μm) and through the bulk of a gemstone (here 6–7 mm).

Raman analysis was conducted with a Renishaw 2000 Raman microspectrometer equipped with a helium/cadmium laser (excitation at 325 nm) and an argon-ion laser (excitation at 514.5 nm). In the absence of polarization accessories, Raman spectra were taken in beam directions oriented nearly parallel and perpendicular to the optic axis of the gemstone.

Quantitative chemical composition was determined by laser ablation–inductively coupled plasma–mass spectrometry (LA-ICP-MS), which is capable of measuring major, minor, and trace elements (see, e.g., Longerich et al., 1996; Günther and Heinrich, 1999). LA-ICP-MS analyses were taken a total of four times, with five ablations (i.e., few-nanogram samples) taken each time for a statistical result. The level of detection that this technique permits is on the order of less than 1 ppm, which makes it much more sensitive than some of the more traditional energy-dispersive chemical analyses techniques, such as SEM-EDS or EDXRF. In addition, a much wider range of elements may be detected than is possible by these other techniques.

TABLE 1. Gemological properties of poudretteite.

Property	Mogok	Mont Saint-Hilaire[a]
Weight	3.00 ct	Not reported (tiny crystals)
Color	Purple-pink	Colorless to very pale pink
Hardness (Mohs scale)	Not tested	Approximately 5
Refractive index	$n_o = 1.511$, $n_e = 1.532$	$n_o = 1.516$, $n_e = 1.532$
Birefringence	0.021	0.016
Optic character	Uniaxial positive	Uniaxial positive
Specific gravity	2.527	2.511 (measured) 2.53 (calculated)
Pleochroism	Strong; saturated purple-pink parallel to the c-axis (o-ray); near-colorless to pale brown perpendicular to the c-axis (e-ray)	Not described
UV fluorescence	Inert	Inert
Visible absorption spectrum	No distinct lines; a faint, broad band centered at approximately 530 nm	Not described

[a]From Grice (1987).

Figure 2. A healed fissure that traverses one side of this extraordinary gemstone consists of equidimensional-to-oblong liquid and liquid-gas inclusions in a parallel formation. Photomicrograph by C. P. Smith; magnified 28×.

RESULTS

Gemological Characteristics. *General Description.* The gemstone weighs 3.00 ct and is fashioned into a cushion shape, with a brilliant-cut crown and a step-cut pavilion. Its measurements are 7.97× 7.91 × 8.62 mm. Face-up, it displays a saturated purple-pink hue (again, see figure 1). However, when the stone is tilted in certain directions, the color appears much less intense (refer to Pleochroism in table 1, and Color Zoning below).

Physical Properties. In table 1, the physical properties are compared to the data previously reported for poudretteite from Quebec. We found no significant differences in the properties of this gem material as

Figure 3. Just below the surface of the stone, oblong and angular negative crystals in the healed fissure are associated with a series of small, parallel fissures. Photomicrograph by C. P. Smith, magnified 32× .

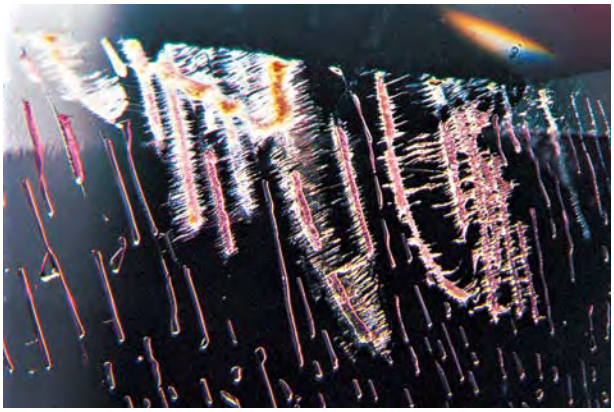

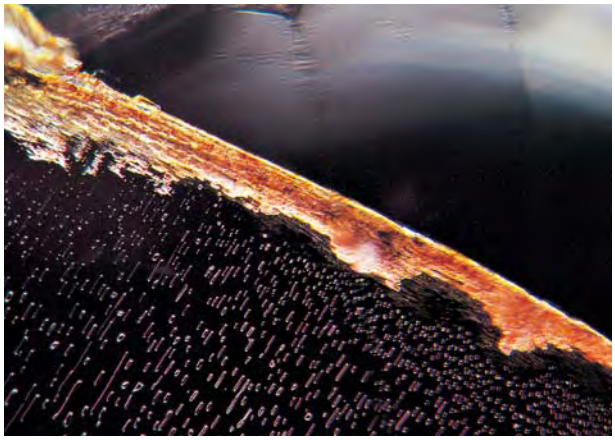

Figure 4. The innermost extension of the healed fissure is delineated by a narrow channel. Clearly evident in this image is the irregular outline and very coarse surface texture of this channel, which is filled with an orange-brown epigenetic material. Photomicrograph by C. P. Smith; magnified 30×.

Figure 5. Very fine growth tubes were also noted in the poudretteite. Here a needle-like growth tube appears doubled as a result of birefringence. Photomicrograph by C. P. Smith; magnified 32×.

compared to those reported for poudretteite from Mont Saint-Hilaire.

Inclusions. The specimen is transparent and gem quality, with only a few inclusions present. One side of the gem is traversed by a healed fissure within which are equidimensional-to-oblong liquid or liquid-gas inclusions (figure 2). Just below the surface, this healed fissure also contains a series of oblong and angular negative crystals that are associated with a series of small fissures all oriented parallel to one another (figure 3). The innermost extension of the healed fissure is delineated by a long, irregular, coarsely textured etch channel that has been filled with an opaque orange-brown material (figure 4). Also present are a few needle-like growth tubes (figure 5) and small aggregates of pinpoint inclusions. A few coarse aggregates of larger crystals (figure 6) were identified as feldspar by Raman analysis.

Figure 6. A few coarse aggregates of small, colorless-to-white crystals in the poudretteite were identified as feldspar. Photomicrograph by C. P. Smith; magnified 70×.

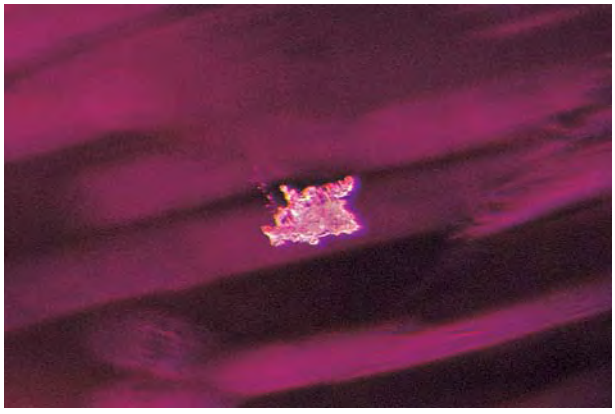

Internal Growth Structures and Color Zoning. When immersed in a near-colorless oil mixture (R.I. ~ 1.51), the poudretteite showed distinct color zoning and growth features parallel to the optic axis (figure 7). An

Figure 7. Distinct color zoning and subtle growth structures were noted in the faceted poudretteite. As evident here in immersion, one stage of the crystal growth is characterized by an intense coloration, with no significant growth structures visible, whereas the outer stages beyond this intense coloration show less uniform, weaker color zoning and more developed growth structures parallel to the prism faces. The irregular outline of the intense color zone corresponds to a period in which the original crystal experienced heavy etching. Photomicrograph by C. P. Smith; magnified 7×.

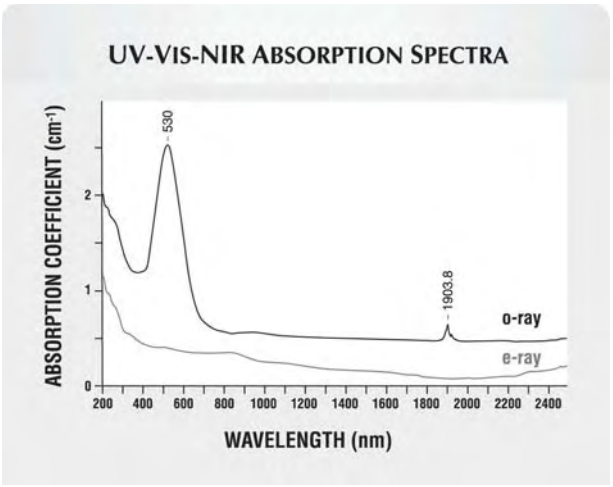

Figure 8. For the "ordinary ray," the UV-Vis-NIR spectrum of the 3 ct poudretteite exhibits a strong and broad absorption band centered at approximately 530 nm and a sharp peak at 1903.8 nm, accompanied by weak sidebands. In the "extraordinary ray" spectrum, these features are completely absent. The dominant absorption band centered at 530 nm in the green region of the visible spectrum is responsible for the intense purple-pink color of the poudretteite. In contrast, the weak absorption slope in the visible region (from 380 to 760 nm) of the e-ray spectrum causes a nearly colorless to pale brown hue in that direction.

intense purple-pink color concentration was present in approximately two-thirds of the stone. No significant growth structures were visible in this highly saturated region. The boundary of this color zone was very irregular but distinct, in that it was closely paralleled by a very narrow, essentially colorless zone. The area of growth adjacent to that zone consisted of a series of planar and angular growth structures that did not repeat the irregular contours of the other two growth zones. These growth planes were oriented parallel to prism faces and consisted of alternating near-colorless and pale purple-pink bands. No twinning or other growth structures were observed.

X-ray Crystallography. A powder diffraction analysis resulted in a distinct pattern of 29 clearly resolved X-ray reflections. The three dominant "lines" are at 5.12, 3.26, and 2.82 Å. The complete X-ray powder diffraction pattern is virtually identical to the type material from Quebec. The unit-cell parameters were refined to be a = 10.245 (2) Å and c = 13.466 (5) Å.

Advanced Analytical Techniques. *UV-Vis-NIR Spectroscopy.* The polarized optical absorption spectra of the poudretteite (figure 8) revealed a very strong, wide band centered at approximately 530 nm for the "ordinary ray" (light vibration perpendicular to the optic axis). In contrast, the "extraordinary ray" (light vibration parallel to the optic axis) showed no 530 nm band but an absorption continuum gradually decreasing from the UV region to the NIR. The 530 nm band is the main color-causing absorption in the visible range of the spectrum. In the near-infrared region (750–2500 nm), we recorded a sharp absorption structure consisting of four bands, with the main band located at 1903.8 nm and very weak side bands at 1898, 1909, and 1911 nm for the ordinary ray. The extraordinary ray did not show any absorption bands in this area. As a result of these different absorption behaviors, the poudretteite displays strong dichroism.

In the UV region, the poudretteite specimen revealed an unfamiliar degree of transparency below 300 nm. Even at 200 nm, the poudretteite

Figure 9. The mid-infrared spectrum of a microsample (<0.001 ct) of poudretteite in a KBr pellet shows the characteristic pattern of poudretteite. The spectral region of approximately 3700–2300 cm^{-1} was corrected for artifacts due to water adsorbed by the KBr pellet and an organic impurity. In the inset, the spectra were recorded with a beam direction parallel and perpendicular to the optic axis of the faceted sample, and show a single absorption band A and the series of bands B, C, and D. The 3659 and 3585 cm^{-1} bands are the only ones to exhibit anisotropic behavior and suggest OH stretching modes.

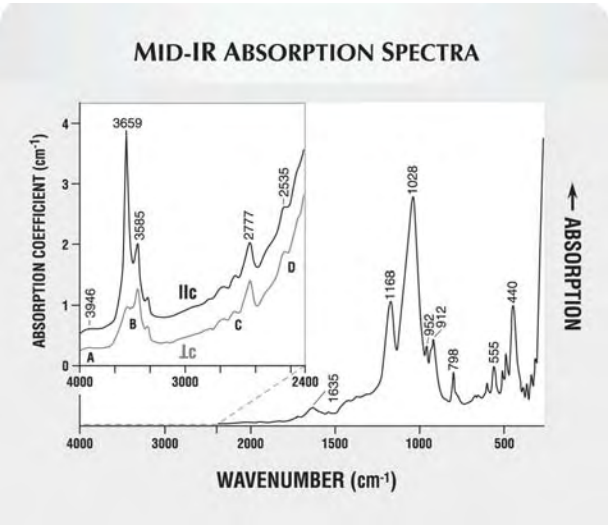

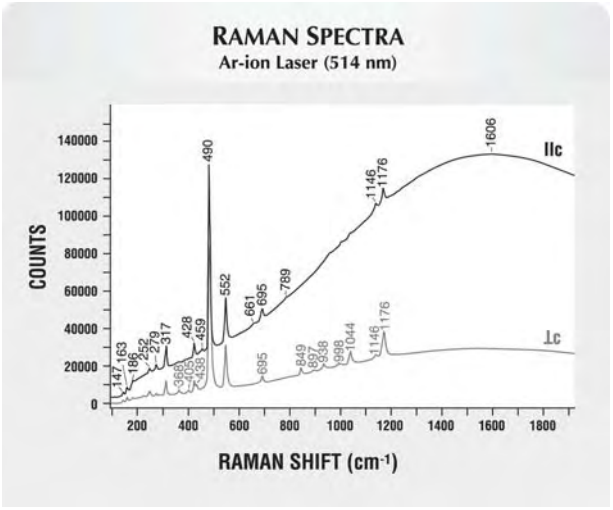

Figure 10. Raman spectra taken with 514 nm laser excitation showed variations in the relative intensities of the three dominant bands present, as well as in some subordinate bands. The dominant peaks for the spectrum taken with the beam direction parallel to the c-axis are at 490, 552, and 317 cm^{-1}; a broad, overlying photoluminescence band centered at about 1500–1600 cm^{-1} masks some of the weaker Raman bands. These weaker bands are clearly seen in the spectrum taken perpendicular to the c-axis, which has dominant peaks at 490, 552, and 1176 cm^{-1}.

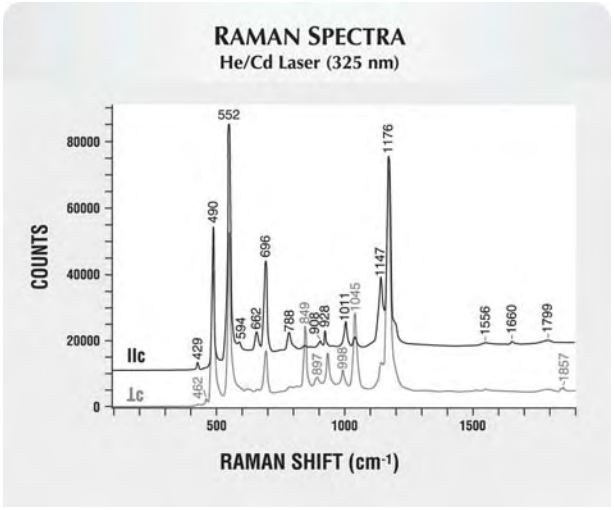

Figure 11. Raman spectra taken with 325 nm laser excitation also showed a change in the relative intensities of the dominant and subordinate bands, with dominant peaks at 552, 1176, and 696 cm^{-1} with the beam direction parallel to the c-axis and at 1176, 490, and 552 cm^{-1} perpendicular to c.

only reached a moderate absorption level but not total absorption.

Mid-Infrared Spectroscopy. The mid-infrared spectrum of poudretteite recorded for the KBr pellet revealed eight dominant bands, as labeled in figure 9, as well as several weaker bands.

Mid-infrared spectra also were recorded for the 3 ct gem with its optic axis oriented as closely parallel and then perpendicular to the infrared beam as possible. Figure 9 (inset) shows the 4000–2400 cm^{-1} region, which is a continuation of the spectra presented in figure 8. A single absorption band and three series of bands were recorded in both spectra, located at (A) 3940 cm^{-1}, (B) 3659, 3630, 3585, 3512 cm^{-1}, (C) 3455, 3380, 3265, 3175, 3080, 2975, 2890, 2777 cm^{-1}, and (D) 2535, 2435 cm^{-1}. The intensity of the bands A, C, and D did not reveal any dependence on the direction of the transmitted IR beam. In contrast, the bands at 3659 and 3585 cm^{-1} in group B exhibited a pronounced anisotropy.

Raman Analysis. In general, the same Raman peaks were present in both spectra recorded with the two lasers. However, their relative intensities varied and, in the case of the spectrum taken with the Ar-ion laser parallel to the c-axis, some Raman bands were masked by a dominant overlying photoluminescence band.

The Raman bands recorded at ambient temperature with the Ar-ion laser are illustrated in figure 10. The three dominant bands (in descending order of intensity) are: 490, 552, and 317 cm^{-1} $\|$c and 490, 552, and 1176 cm^{-1} $\perp$c. The Raman bands recorded with the He/Cd laser are illustrated in figure 11. The three dominant bands are 552, 1176, and 696 cm^{-1} $\|$c and 1176, 490, and 552 cm^{-1} $\perp$c.

Chemical Analysis. Of the four analyses taken, two were performed in the highly saturated region and two in the colorless to near-colorless region. Statistically, all analyses were highly consistent with regard to major elements: SiO_2 (78.99 wt.%), B_2O_3 (10.53–11.03 wt.%), Na_2O (6.20–6.53 wt.%), and K_2O (3.45–4.09 wt.%). These major-element concentrations are in good agreement with the data obtained by Grice et al. (1987): SiO_2 (77.7 wt.%), B_2O_3 (11.4 wt.%), Na_2O (6.2 wt.%), K_2O (5.2 wt.%). In addition, more than 30 other elements were measured (ranging from Li to U). Of these, 21 trace elements were detected at the ppm (parts per million) level. Two of these trace elements displayed a consistently higher concentration in the saturated

region as compared to the near-colorless one: Li (14 ppm and 9–10 ppm, respectively) and Mn (49–52 ppm and 16–21 ppm). Others revealed an opposite correlation: Ca (32–55 ppm and 79–132 ppm, respectively), Rb (83–86 ppm and 112–114 ppm), and Cs (8 ppm and 9–10 ppm). Be, Mg, Al, Ti, V, Cr, Fe, Ni, Cu, Zn, Ga, Sr, Zr, Sn, Pb, and Bi revealed a high degree of variability but no apparent correlation between the different color regions.

DISCUSSION AND SUMMARY

It is likely that few gemologists will ever encounter a faceted poudretteite. The combination of refractive indices and specific gravity will readily separate it from amethyst, which is probably the only major commercially available gem material that it might be confused with. However, the visual appearance/color of poudretteite is also significantly different from that of amethyst. Poudretteite might also be confused with sugilite, some of which is translucent (as opposed to the typically encountered opaque material) and has been polished *en cabochon* and even rarely faceted (Shigley et al., 1987). Although the color of these two materials is more similar, poudretteite is a transparent mineral, while sugilite is, even in its best quality, translucent. In addition, the refractive index (approximately 1.60) and specific gravity (ranging from 2.74 to 2.80) of sugilite are significantly higher than that of poudretteite.

The main color-causing absorption centered at 530 nm is not yet fully understood and requires further analytical investigation. However, we can discuss potential mechanisms based on the trace-element composition. Manganese is the primary color-causing element of the similarly colored member of the osumilite/milarite group, sugilite, which has a dominant broad absorption band at approximately 556 nm (see, e.g., Shigley et al., 1987). It is not surprising that there was considerable variation in Mn concentration between the near-colorless and highly saturated areas of the poudretteite (averaging 16–21 ppm and 49–52 ppm, respectively, although this is surprisingly low for so intense a color). Substitution of cations by divalent and trivalent transition metal ions is the most frequent cause of color in silicates. Manganese (as Mn^{2+} or Mn^{3+}) is a common cause of pink to red and purple coloration in a variety of other gem-quality silicate minerals, such as red beryl and tourmaline, as well as the carbonate rhodochrosite (see, e.g., Fritsch and Rossman, 1987, 1988). However, other trace elements or possibly color centers may also have an influence in producing the intense purple coloration.

The intensity of the group B peaks in the mid-infrared region (again, see figure 9 inset) differ when recorded parallel and perpendicular to the optic axis. This indicates that the 3659 and 3585 cm^{-1} bands are anisotropic. These bands suggest OH stretching. In addition, the 1635 cm^{-1} band indicates H_2O bending, and the band structure centered at 1903.8 nm (5253 cm^{-1}) represents the combination of these stretching and bending modes (E. Libowitzky, pers. comm., 2003). Within poudretteite, H_2O molecules are likely to be positioned in the channels of the ring silicate structure.

As would be expected for a uniaxial mineral, the Raman spectra of poudretteite are polarized parallel and perpendicular to the c-axis. This includes a change in the relative intensities of the three dominant bands, as well as variations in several subordinate bands. In addition, depending on which laser was used to obtain the Raman signal, distinct differences in the three dominant peaks were identified when measurements were taken parallel to the c-axis direction, whereas only slight variations in relative peak intensities were noted for the measurements taken perpendicular to the c-axis.

The chemical composition determined by LA-ICP-MS for the study sample is in good agreement with previous chemical data reported by Grice et al. (1987). However, the list of elements has been significantly extended by several trace elements present at concentrations as low as 1 ppm.

Not unlike the unique alkali gabbro-syenite geology of the Mont Saint-Hilaire region, the complex geology of the Mogok Stone Tract has also produced a special environment for the prolific growth of minerals of sufficient size and transparency that they can be considered gem quality. Contact and regional metamorphism in the Mogok area is well known for providing the geologic environment for rare gems to form (e.g., painite), and the region plays host to a wide variety of gem materials, including many silicates.

CONCLUSION

Gemologists continue to be excited by the discovery of minerals that have never before been seen in a transparency and size suitable for faceting (see, e.g., McClure, 2002; Schmetzer et al., 2003). When such

rarities are encountered, they present unique opportunities to expand the science of gemology and mineralogy. Such is the case with the recent identification of the faceted 3.00 ct intense purple-pink specimen of poudretteite from Myanmar. Prior to this find, the seven crystals of poudretteite known to exist were small, pale in color, and came from a single quarry in Quebec, Canada, during the 1960s.

The data obtained during this study are in agreement with those documented by past researchers for poudretteite from Canada. In addition to confirming the standard physical/gemological properties of this mineral, analysis of this gemstone also permitted the authors to significantly expand the documentation of poudretteite, specifically in terms of its spectral characterization and chemical composition.

ABOUT THE AUTHORS

Mr. Smith is managing director, and Mr. Bosshart is chief gemologist, at the Gübelin Gem Lab Ltd., Lucerne, Switzerland. Dr. Graeser is a semi-retired professor of mineralogy at the Institute of Mineralogy and Petrography, University of Basel, Switzerland. Dr. Hänni is head of the SSEF Swiss Gemmological Institute, Basel. Dr. Günther is assistant professor of analytical chemistry, and Ms. Hametner is operator of the laser ablation system in the Laboratory of Inorganic Chemistry, at the Swiss Federal Institute of Technology (ETH), Zurich. Dr. Gübelin is a noted gemological researcher residing in Lucerne.

ACKNOWLEDGMENTS

The authors thank Federico Barlocher, Lugano, Switzerland, for submitting the 3.00 ct poudretteite for identification and permitting us to publish the results of our research. The following kindly provided fruitful discussions: Dr. A. A. Levinson of the University of Calgary, Canada; Prof. Eugen Libowitzky of the University of Vienna, Austria; and Dr. Joel Grice, research scientist, Canadian Museum of Nature, Ottawa, Canada.

REFERENCES

Bank H., Banerjee A., Pense J., Schneider W., Schrader W. (1978) Sogdianit-ein neues Edelsteinmineral? *Zeitschrift der Deutschen Gemmologischen Gesellschaft*, Vol. 27, No. 2, pp. 104–105.

Benoit P. (1987) Adaptation to microcomputer of the Appleman-Evans program for indexing and least-squares refinement of powder-diffraction data for unit-cell dimensions. *American Mineralogist*, Vol. 72, No. 9/10, pp. 1018–1019.

Clark M.A. (1993) *Hey's Mineral Index* (3rd ed.). Chapman & Hall, London, 852 pp.

Dillman R. (1978) Sogdianit. *Zeitschrift der Deutschen Gemmologischen Gesellschaft*, Vol. 27, No. 4, p. 214.

Fritsch E., Rossman G.R. (1987) An update on color in gems. Part 1: Introduction and colors caused by dispersed metal ions. *Gems & Gemology*, Vol. 23, No. 3, pp. 126–139.

Fritsch E., Rossman G.R. (1988) An update on color in gems. Part 3: Colors caused by band gaps and physical phenomena. *Gems & Gemology*, Vol. 24, No. 2, pp. 81–102.

Grice J.D., Ercit T.S., van Velthuizen J., Dunn P.J. (1987) Poudretteite, $KNa_2B_3Si_{12}O_{30}$, A new member of the osumilite group from Mont Saint-Hilaire, Quebec, and its crystal structure. *Canadian Mineralogist*, Vol. 25, No. 4, pp. 763–766.

Günther, D. and Heinrich, C.A. (1999) Enhanced sensitivity in LA-ICP-MS using helium-argon mixtures as aerosol carrier. *Journal of Analytic Atomic Spectrometry*, Vol. 14, No. 9, pp. 1363–1368.

Hawthorne F.C., Grice J.D. (1990) Crystal-structure analysis as a chemical analytical method: Application to light elements. *Canadian Mineralogist*, Vol. 28, Part 4, pp. 693–702.

Hawthorne F.C., Kimata M., Černý P., Ball N., Rossman G.R., Grice J.D. (1991) The crystal chemistry of the milarite-group minerals. *American Mineralogist*, Vol. 76, No. 11/12, pp. 1836–1856.

Holland T.J.B., Redfern S.A.T. (1997) Unit cell refinement from powder diffraction data: The use of regression diagnostics. *Mineralogical Magazine*, Vol. 61, No. 1, pp. 65–77.

Kammerling R.C., Scarratt K., Bosshart G., Jobbins E.A., Kane R.E., Gübelin E.J., Levinson A.A. (1994) Myanmar and its gems—An update. *Journal of Gemmology*, Vol. 24, No. 1, pp. 3–40.

Kiefert L., Schmetzer K. (1991) The microscopic determination of structural properties for the characterization of optical uniaxial natural and synthetic gemstones. Part 1: General considerations and description of the methods. *Journal of Gemmology*, Vol. 22, No. 6, pp. 344–354.

Longerich H.P., Jackson S.E., Günther D. (1996) Laser ablation inductively coupled plasma mass spectrometry transient signal data acquisition and analyte concentration calculation. *Journal of Analytic Atomic Spectrometry*, Vol. 11, No. 9, pp. 899–904.

Mandarino J.A. (1999) *Fleischer's Glossary of Mineral Species*. Mineralogical Record, Tucson, Arizona, 235 pp.

McClure S.F. (2002) Gem Trade Lab notes: Bromellite. *Gems & Gemology*, Vol. 38, No. 3, pp. 250–252.

Schlüssel R. (2002) *Mogok, Myanmar. Eine Reise durch Burma zu den schönsten Rubinen und Saphiren der Welt*. Christian Weise Verlag, Munich, 280 pp.

Schmetzer K., Burford M., Kiefert L., Bernhardt H.-J. (2003) The first transparent faceted grandidierite, from Sri Lanka. *Gems & Gemology*, Vol. 39, No. 1, pp 32–37.

Shigley J.E., Koivula J.I., Fryer C.W. (1987) The occurrence and gemological properties of Wessels mine sugilite. *Gems & Gemology*, Vol. 23, No. 2, pp. 78–89.

Smith C.P. (1996) Introduction to analyzing internal growth structures: Identification of the negative d plane in natural ruby. *Gems & Gemology*, Vol. 32, No. 3, pp. 170–184.

Themelis T. (2000) *Mogok—Valley of Rubies & Sapphires*. A & T Publishing, Los Angeles, 270 pp.